

## Deformation and stress analysis of rotating functionally graded hollow cylindrical body for variable heat generation

Rakesh Kumar Sahu, Lakshman Sondhi, Shubhankar Bhowmick, Royal Madan

Online Publication Date: 20 Dec 2022

URL: <http://www.jresm.org/archive/resm2022.470me0713.html>

DOI: <http://dx.doi.org/10.17515/resm2022.470me0713>

### To cite this article

Sahu RK, Sondhi L, Bhowmick S, Madan R. Deformation and stress analysis of rotating functionally graded hollow cylindrical body for variable heat generation. *Res. Eng. Struct. Mater.*, 2023; 9(2): 597-616.

### Disclaimer

All the opinions and statements expressed in the papers are on the responsibility of author(s) and are not to be regarded as those of the journal of Research on Engineering Structures and Materials (RESM) organization or related parties. The publishers make no warranty, explicit or implied, or make any representation with respect to the contents of any article will be complete or accurate or up to date. The accuracy of any instructions, equations, or other information should be independently verified. The publisher and related parties shall not be liable for any loss, actions, claims, proceedings, demand or costs or damages whatsoever or howsoever caused arising directly or indirectly in connection with use of the information given in the journal or related means.



Published articles are freely available to users under the terms of Creative Commons Attribution - NonCommercial 4.0 International Public License, as currently displayed at [here](https://creativecommons.org/licenses/by-nc/4.0/) (the "CC BY - NC").



## Deformation and stress analysis of rotating functionally graded hollow cylindrical body for variable heat generation

Rakesh Kumar Sahu<sup>1,a</sup>, Lakshman Sondhi<sup>1,b</sup>, Shubhankar Bhowmick<sup>2,c</sup>,  
Royal Madan<sup>\*3,d</sup>

<sup>1</sup>Department of Mechanical Engineering, Shri Shankaracharya Group of Institute, Bhilai, India

<sup>2</sup>Department of Mechanical Engineering, National Institute of Technology Raipur, Raipur, India

<sup>3</sup>Department of Mechanical Engineering, G H Raisoni Institute of Engineering & Technology, Nagpur, India

### Article Info

### Abstract

#### Article history:

Received 13 Jul 2022

Revised 14 Oct 2022

Accepted 12 Dec 2022

#### Keywords:

Functionally graded materials;

Stress analysis;

Hollow cylinder;

Navier's method

In the present study, one-dimensional steady-state temperature variation with variable heat generation was considered and thermo-mechanical stress and deformation analysis on a hollow functionally graded cylinder were then performed. A governing differential equation with a variable coefficient is solved using Navier's equation by applying thermal and mechanical boundary conditions. The effect of internal pressure and temperature, rotation, gravity, and heat generation, and their combined effect such as rotation and heat generation, gravity and heat generation, rotation, gravity, and heat generation were studied in a cylindrical body. The gradation properties varied radially as per power-law variation. The grading parameter ranging between -2 to 3, changes the material properties in the radial direction. A critical grading index was identified that lowers the induced stresses and hence an improvement in the performance of functionally graded cylinders can be obtained under the influence of a combination of loads. The validation of the results was carried out with published literature.

© 2022 MIM Research Group. All rights reserved.

## 1. Introduction

In functionally graded materials (FGM) the properties change with distance because of changes in composition, microstructure, or porosity gradient [1]. The change in composition can be stepped-wise or continuously varying depending on the fabrication route selected, for ex., a layer-wise FGM is obtained in the case of powder metallurgy and continuously varying type in centrifugal casting [2]. Mainly the choice of functionally graded material selected is a combination of a metal-ceramic type wherein the metal provides the toughness and ceramic the wear resistance, therefore, the structure then obtained has potential applications in areas like nuclear energy, defense, biomedical, aerospace, energy-based, semiconductor, and cutting tools to name a few [3]. Various methods are available for the fabrication of FGMs such as solid-based, liquid-based, and gas-based, but for the fabrication of axisymmetric structures, a centrifugal casting method was found to be an effective fabrication technique [4–6]. To ascertain the performance of such structures, a prior analysis would be advantageous, as it saves costs, time, and other resources. Hence, modeling and analysis of structures (Plate, shell, disk, and cylinder) are of interest to researchers [7–9]. There are two approaches to model the properties of functionally graded materials; in the first approach, the material properties are varied based on the volume fraction variation of metal and ceramic. The variation of

\*Corresponding author: [royalmadan6293@gmail.com](mailto:royalmadan6293@gmail.com)

<sup>a</sup> [orcid.org/0000-0002-9794-722X](https://orcid.org/0000-0002-9794-722X); <sup>b</sup> [orcid.org/0000-0002-5259-2218](https://orcid.org/0000-0002-5259-2218); <sup>c</sup> [orcid.org/0000-0001-9799-8724](https://orcid.org/0000-0001-9799-8724);

<sup>d</sup> [orcid.org/0000-0002-3445-9210](https://orcid.org/0000-0002-3445-9210)

DOI: <http://dx.doi.org/10.17515/resm2022.470me0713>

Res. Eng. Struct. Mat. Vol. 9 Iss. 2 (2023) 597-616

volume fraction variation can be as per laws like power-law, exponential law, and sigmoid law [10] or by assuming a variation of properties like exponentially, power-law, and others. The effective estimation of the mechanical property of the material in which the volume fraction changes can be carried out using methods such as rule of mixture, modified rule of mixture, Mori-Tanaka, and others [11].

Cylindrical structures are employed in a wide range of engineering applications, including marine, reactor, rocket components, and automotive, to name a few [12]. When compared to isotropic material, a functionally graded cylinder has a larger energy absorption capacity [13, 14]. A nonlinear finite element approach was employed to study buckling in a cylindrical panel for several lamination arrangements and boundary conditions [15]. The pressure-bearing capability of shells under blast loading was solved using Lamé's approach [16]. Elastic-plastic stress analysis of an FG solid cylinder subjected to homogenous heat generation was performed based on Tresca's yield criteria [17]. Under uniform internal pressure, the complementary functions approach was used to investigate stress distribution in hollow cylinders, disks, and spheres [18]. Finite element analysis has been employed to investigate the temperature distribution in a wet cylinder liner and bonded T-joints [19, 20]. Free vibration and buckling analysis of functionally graded beams were performed using the finite element approach [21]. Analytical and experimental analysis of an isotropic material was carried out to investigate the yield criteria of plasticity models [22].

The power series method was used to calculate displacements and stresses in an exponentially graded thick cylinder under internal pressure [23]. For variable thickness, a cylindrical shell under internal pressure was considered to perform stress analysis using first-order shear deformation theory (FSDT) [24]. The Bessel function was used to develop a closed-form solution of an FG hollow cylinder exposed to thermo-mechanical loading assuming steady-state temperature distribution along the radial and longitudinal directions [25]. The energy method was used in an FG piezoelectric rotating cylinder under the influence of electrical, thermal, and mechanical loads [26]. For the FG pressure vessel, an analytical solution for non-uniform pressure loading was solved using FSDT [27]. The FG rotating thick cylinder shell problem was addressed using a multi-layered approach under arbitrary non-uniform internal pressure [28]. In [29], investigated the hollow cylinder problem in two different ways: Firstly, the hollow cylinder is made of a multi-layered material with variable material properties on each layer; the material properties in the second case were continually changing. A closed-form solution to the exponentially graded hollow cylinder problem was used to investigate stress distribution under thermo-mechanical loads [30]. By employing Fredholm's integral equation thermal stresses and displacement of a functionally graded cylindrical vessel were studied [31]. An elasto-plastic thermo-mechanical analysis of a thick-walled cylinder when subjected to internal pressure and the temperature has been performed using the Successive Approximation Method, and they found that the effect of boundary temperature on radial and tangential stress is insignificant [32]. Thermo-mechanical fatigue analysis and failure location in the cylinder head were investigated [33]. A fast Fourier transform and finite element method were combinely employed in the thermo-mechanical analysis of a thick cylinder [34]. Elastic analysis of a thick cylinder and spherical pressure vessel made up of functionally graded material (FGM) was studied and found a significant reduction in stresses when compared with homogeneous material [35]. Finite element analysis has been employed to analyze the thermo-elastic analysis of a rotating FGM circular disk [36]. A lot of research in the fabrication and analysis of functionally graded structures is going on. Studies on static and dynamic analysis on FGM plates have been performed by authors using methods such as higher-order shear deformation theory [37–39], and sinusoidal shear deformation [40] to name a few.

In this paper, using Navier’s equation a thermal and mechanical analysis of a rotating FG hollow cylinder was performed. Considering one-dimensional steady-state thermal heat conduction, stress and deformation analysis were performed when a cylinder is subjected to combined thermal and rotational effects. For property variation in a radial direction, the individual and combined effects of rotation, gravity, and heat generation on stresses: radial, tangential, and von Mises were investigated. To the best of the author’s knowledge, there is no study in which the effect of variable heat generation on stresses is considered, such situations are practical in the case of functionally graded materials. The material properties of FGMs such as Young’s modulus, density, coefficient of thermal expansion, conductivity, and heat generation was considered as per power law variation. The proposed method is simple and validated with benchmark solutions. The study will benefit researchers and industries in understanding the effects of individual loadings and the combination of them such as gravity, rotation, and variable heat generation. Thus, the research will help industry personnel in selecting suitable grading parameters for different cases before the fabrication of such structures.

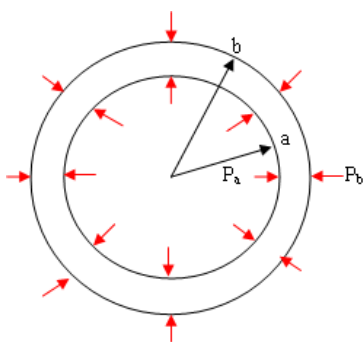


Fig. 1 Hollow cylinder

**2. Mathematical Formulation**

A rotating hollow cylinder is considered whose inner and outer radius are ‘a’ and ‘b’. Variation of material properties of rotating hollow cylinder is a function of radial direction ‘r’. Let displacement component ‘u’ is the function of radial direction. The displacement relation for combined thermal and mechanical strain is given by;

$$\epsilon_r = \frac{du}{dr} = \frac{1}{E_r} [\sigma_r - \nu\sigma_\theta] + \alpha_r T_r \quad \text{and} \quad \epsilon_\theta = \frac{u}{r} = \frac{1}{E_r} [\sigma_\theta - \nu\sigma_r] + \alpha_r T_r \tag{1}$$

The stress-strain relations are given by,

$$\sigma_r = \frac{E_r}{(1+\nu)(1-2\nu)} [\epsilon_r(1-\nu) + \nu\epsilon_\theta - (1+\nu)\alpha_r T_r] \tag{2}$$

$$\sigma_\theta = \frac{E_r}{(1+\nu)(1-2\nu)} [\nu\epsilon_r + (1-\nu)\epsilon_\theta - (1+\nu)\alpha_r T_r]$$

Concerning the body force and inertia term the equation thus becomes,

$$r \frac{d}{dr} \sigma_r + (\sigma_r - \sigma_\theta) + \rho_r \left( \omega^2 - \frac{g}{a} \right) r^2 = 0 \tag{3}$$

By employing the power law in the material properties, we get;

$$E_r = E_a(r)^{n_1}, \alpha_r = \alpha_a(r)^{n_2}, k_r = k_a(r)^{n_3}, \rho_r = \rho_a(r)^{n_4}, q_r = q_a(r)^{n_5} \tag{4}$$

Solving Eq. (1-4), the displacement formulation thus becomes

$$r \frac{d}{dr} \left[ E_r \lambda \left\{ (1-\vartheta) \frac{du}{dr} + \vartheta \frac{u}{r} - (1+\vartheta) \alpha_r T_r \right\} \right] + E_r \lambda \left[ (1-\vartheta) \frac{du}{dr} + \vartheta \frac{u}{r} - (1+\vartheta) \alpha_r T_r \right] - E_r \lambda \left[ \vartheta \frac{du}{dr} + (1-\vartheta) \frac{u}{r} - (1+\vartheta) \alpha_r T_r \right] + \rho_r (\omega^2 - \frac{g}{a}) r^2 = 0 \tag{5}$$

where,

$$\lambda = \frac{1}{(1+\vartheta)(1-2\vartheta)} \tag{6}$$

Above eq. (5) can also be written as here we required the values for temperature and its derivative. The formulation for the temperature profile is separately calculated in section 2.1

$$Ar^2u'' + Bru' + Cu = Ur^{n_2+P_4+1} + Vr^{n_2-n_3+n_5+3} + Wr^{n_2+1} + Sr^{n_4-n_1+3} \tag{7}$$

where,

$$A = E_a \lambda (1-\vartheta), B = n_1 E_a \lambda (1-\vartheta) + E_a \lambda (1-\vartheta), C = E_a \lambda \vartheta n_1 + E_a \lambda \vartheta - E_a \lambda$$

$$U = \frac{1}{(1-2\vartheta)} [E_a \alpha_a Q_4 P_4 + E_a \alpha_a Q_4 n_1 + E_a \alpha_a Q_4 n_2], V = \frac{\beta_1 E_a \alpha_a}{(1-2\vartheta)} [n_5 - n_3 + n_1 + n_2 + 2]$$

$$W = \frac{Q_3 E_a \alpha_a}{(1-2\vartheta)} [n_1 + n_2], S = -\rho_a \left[ \omega^2 - \left( \frac{g}{a} \right) \right] \tag{8}$$

### 2.1 Temperature Formulation

A one-dimensional steady-state heat conduction equation includes variable conductivity and temperature variation.

$$\frac{1}{r} \frac{d}{dr} \left[ r k_r \frac{d}{dr} (T_r) \right] + q_r = 0 \tag{9}$$

And boundary conditions for thermal are given by,

$$T_r = T_a \text{ at } r = a \text{ and } T_r = T_b \text{ at } r = b \tag{10}$$

Differentiating the above eq.(9) of the heat conduction equation to obtain the Navier equation for temperature,

$$A_1 r^2 T_r'' + B_1 r T_r' + C_1 T_r = \gamma_1 r^{n_5-n_3+2} \tag{11}$$

where

$$A_1 = k_a, B_1 = k_a(n_3+1), C_1 = 0, \gamma_1 = -q_a$$

After solving eq.(11),

$$T_r = Q_3 + Q_4 r^{P_4} + \beta_1 r^{n_5 - n_3 + 2}, \quad \frac{dT}{dr} = Q_4 P_4 r^{P_4 - 1} + \beta_1 (n_5 - n_3 + 2) r^{n_5 - n_3 + 1} \tag{12}$$

$$P_3 = 0, \quad P_4 = \frac{A_1 - B_1}{A_1} = -n_3$$

Using the boundary condition find-out the value of  $Q_3$  and  $Q_4$  yields,

$$Q_4 = \frac{T_a - T_b}{a^{P_4} - b^{P_4}} - \frac{\beta_1 (a^{n_5 - n_3 + 2} - b^{n_5 - n_3 + 2})}{a^{P_4} - b^{P_4}} \quad \text{and} \quad Q_3 = T_a - \beta_1 a^{n_5 - n_3 + 2} - Q_4 a^{P_4} \tag{13}$$

### 2.2 Solution of Displacement Equation

The displacement formulation has a general solution and a particular solution. Now general part of the solution,  $u_g$  is obtained by assuming,

$$u_g = Qr^P \tag{14}$$

Substitute the above eq.(14) in the homogeneous form of eq.(7) to get,

$$AP^2 + (B - A)P + C = 0 \tag{15}$$

The above eq. (15) has 2 real roots  $P_1$  and  $P_2$  as,

$$P_{1,2} = \frac{(A - B) \pm \sqrt{(B - A)^2 - 4AC}}{2A} \tag{16}$$

Thus, the general solution is,

$$u_g = Q_1 r^{P_1} + Q_2 r^{P_2} \tag{17}$$

Now particular part of the solution  $u_p$  is assumed to have the form

$$u_p = I r^{n_2 + P_4 + 1} + J r^{n_2 - n_3 + n_5 + 3} + L r^{n_2 + 1} + M r^{n_4 - n_1 + 3} \tag{18}$$

Solving, we get,

$$\begin{aligned} & [A(n_2 + P_4 + 1)(n_2 + P_4) + B(n_2 + P_4 + 1) + C] I r^{n_2 + P_4 + 1} + \\ & [A(n_2 + n_5 - n_3 + 3)(n_2 + n_5 - n_3 + 2) + B(n_2 + n_5 - n_3 + 3) + C] J r^{n_2 - n_3 + n_5 + 3} \\ & + [A(n_2 + 1)n_2 + B(n_2 + 1) + C] L r^{n_2 + 1} + [A(n_4 - n_1 + 3)(n_4 - n_1 + 2) + B(n_4 - n_1 + 3) + C] M r^{n_4 - n_1 + 3} \\ & = U r^{n_2 + P_4 + 1} + V r^{n_2 - n_3 + n_5 + 3} + W r^{n_2 + 1} + S r^{n_4 - n_1 + 3} \end{aligned} \tag{19}$$

On solving the above equation, the following form is obtained.

$$\begin{aligned}
 I &= \frac{U}{A[(n_2 + P_4 + 1)(n_2 + P_4)] + B[n_2 + P_4 + 1] + C} \\
 J &= \frac{V}{A[(n_2 + n_5 - n_3 + 3)(n_2 + n_5 - n_3 + 2)] + B[(n_2 - n_3 + n_5 + 3)] + C} \\
 L &= \frac{W}{A[(n_2 + 1)(n_2)] + B[(n_2 + 1)] + C} \\
 M &= \frac{S}{A[(n_4 - n_1 + 3)(n_4 - n_1 + 2)] + B[(n_4 - n_1 + 3)] + C}
 \end{aligned}
 \tag{20}$$

Now the complete solution 'u' is the sum of the general part of the solution and the particular part of the solution as,

$$u = u_g + u_p \tag{21}$$

Thus,

$$u = Q_1 r^{P_1} + Q_2 r^{P_2} + I r^{n_2 + P_4 + 1} + J r^{n_2 - n_3 + n_5 + 3} + L r^{n_2 + 1} + M r^{n_4 - n_1 + 3} \tag{22}$$

Substituting eq.(22) in eq.(1) and (2), the stress and strain distributions can be written as,

$$\begin{aligned}
 \epsilon_r &= Q_1 P_1 r^{P_1 - 1} + Q_2 P_2 r^{P_2 - 1} + I(n_2 + P_4 + 1)r^{n_2 + P_4} + J(n_2 - n_3 + n_5 + 3)r^{n_2 - n_3 + n_5 + 2} \\
 &+ L(n_2 + 1)r^{n_2} + M(n_4 - n_1 + 3)r^{n_4 - n_1 + 2}
 \end{aligned}
 \tag{23}$$

$$\epsilon_\theta = Q_1 r^{P_1 - 1} + Q_2 r^{P_2 - 1} + I r^{n_2 + P_4} + J r^{n_2 - n_3 + n_5 + 2} + L r^{n_2} + M r^{n_4 - n_1 + 2} \tag{24}$$

$$\begin{aligned}
 \sigma_r &= E_a \lambda \left[ \begin{aligned}
 &Q_1 \{ (1 - \vartheta) P_1 + \vartheta \} r^{n_1 + P_1 - 1} + Q_2 \{ (1 - \vartheta) P_2 + \vartheta \} r^{n_1 + P_2 - 1} + I r^{n_1 + n_2 + P_4} \{ (1 - \vartheta)(n_2 + P_4 + 1) + \vartheta \} + \\
 &J r^{n_1 + n_2 + n_5 - n_3 + 2} \{ (1 - \vartheta)(n_2 + n_5 - n_3 + 3) + \vartheta \} + L r^{n_1 + n_2} \{ (1 - \vartheta)(n_2 + 1) + \vartheta \} + \\
 &M r^{n_1 + 2} \{ (1 - \vartheta)(n_4 - n_1 + 3) + \vartheta \} - (1 + \vartheta) \alpha_a \{ Q_3 r^{n_1 + n_2} + Q_4 r^{n_1 + n_2 + P_4} + \beta_1 r^{n_1 + n_2 + n_5 - n_3 + 2} \}
 \end{aligned} \right]
 \end{aligned}
 \tag{25}$$

The boundary condition of stresses is used to determine the constant  $Q_1$  and  $Q_2$ . Considering the mechanical boundary condition on the inner side and outer side surface of the cylinder as

$$\sigma_r = -P_a \text{ at } r = a \text{ and } \sigma_r = -P_b \text{ at } r = b \tag{26}$$

Substituting the stress boundary condition in eq.(25), the constants become,

$$Q_1 = \frac{\phi_{22} X - \phi_{12} Y}{\phi_{11} \phi_{22} - \phi_{12} \phi_{21}} \text{ and } Q_2 = \frac{\phi_{11} Y - \phi_{21} X}{\phi_{11} \phi_{22} - \phi_{12} \phi_{21}} \tag{27}$$

$$\begin{aligned}
 \phi_{11} &= E_a \lambda [P_1(1 - \nu) + \nu] a^{n_1 + P_1 - 1} & \phi_{12} &= E_a \lambda [P_2(1 - \nu) + \nu] a^{n_1 + P_2 - 1} \\
 \phi_{21} &= E_a \lambda [P_1(1 - \nu) + \nu] b^{n_1 + P_1 - 1} & \phi_{22} &= E_a \lambda [P_2(1 - \nu) + \nu] b^{n_1 + P_2 - 1}
 \end{aligned}
 \tag{28}$$

$$X = -Z(a) - P_a, \quad Y = -Z(b) - P_b \tag{29}$$

$$Z(a) = E_a \lambda \left[ \begin{aligned} &Ia^{n_1+n_2+P_4} \{(1-\varrho)(n_2+P_4+1)+\varrho\} + Ja^{n_1+n_2+n_5-n_3+2} \{(1-\varrho)(n_2+n_5-n_3+3)+\varrho\} \\ &+ La^{n_1+n_2} \{(1-\varrho)(n_2+1)+\varrho\} + Ma^{n_4+2} \{(1-\varrho)(n_4-n_1+3)+\varrho\} \\ &- (1+\varrho)\alpha_a \{Q_3a^{n_1+n_2} + Q_4a^{n_1+n_2+P_4} + \beta_1a^{n_1+n_2+n_5-n_3+2}\} \end{aligned} \right] \quad (30)$$

$$Z(b) = E_a \lambda \left[ \begin{aligned} &Ib^{n_1+n_2+P_4} \{(1-\varrho)(n_2+P_4+1)+\varrho\} + Jb^{n_1+n_2+n_5-n_3+2} \{(1-\varrho)(n_2+n_5-n_3+3)+\varrho\} + \\ &Lb^{n_1+n_2} \{(1-\varrho)(n_2+1)+\varrho\} + Mb^{n_4+2} \{(1-\varrho)(n_4-n_1+3)+\varrho\} \\ &- (1+\varrho)\alpha_a \{Q_3b^{n_1+n_2} + Q_4b^{n_1+n_2+P_4} + \beta_1b^{n_1+n_2+n_5-n_3+2}\} \end{aligned} \right] \quad (31)$$

### 3. Result and Discussion

#### 3.1 Functionally Graded Properties

The variation in material parameters such as Young’s modulus of elasticity, thermal expansion coefficient, density, and thermal conductivity along the cylinder radius is shown in Fig. 2 to Fig. 5. When the grading parameter (**n**) is zero it represents isotropic material behaviour. When the grading parameter (**n**) is positive the material properties increase as the radius increases, whereas when the parameter (**n**) is negative the material properties decrease as the radius increases.

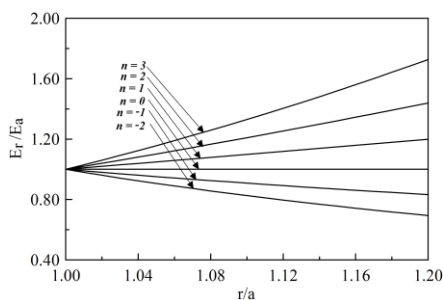


Fig. 2 Young’s modulus variation

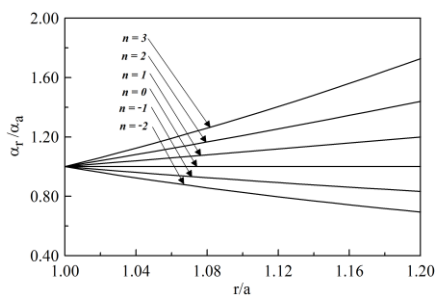


Fig. 3 Thermal expansion coefficient

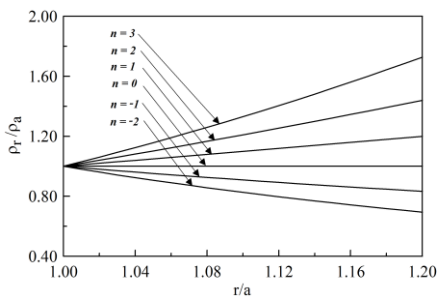


Fig. 4 Density variation

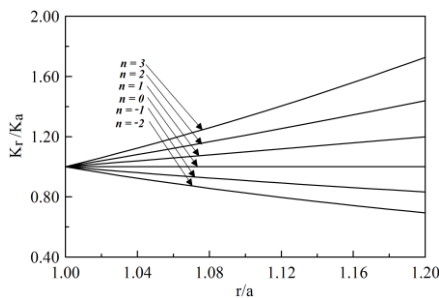


Fig. 5 Thermal conduction coefficient

### 3.2 Validation

Table 1. Geometrical and mechanical properties

Physical properties		Material properties						Boundary condition			
$a$	$b$	$E_a$	$\alpha_a$	$k_a$	$\rho_a$	$q_a$	$\vartheta$	$P_a$	$P_b$	$T_a$	$T_b$
$m$	$m$	GPa	per °C	W/mk	kg/m <sup>3</sup>	kJ/m <sup>3</sup>		MPa	MPa	°C	°C
1	1.2	200	1.2*10 <sup>-6</sup>	15	7800	50*10 <sup>3</sup>	0.3	50	0	10	0

The grading index  $n_1 = n_2 = n_3 = n_4 = n_5 = n$  is selected as -2 to 3 and the results of the present method are compared with the literature [41]. Because for this particular range of  $n$ , the composition of metal and ceramic in a functionally graded material is a desired one. Beyond this range of  $n$ , an FGM would have an excessive amount of one phase, which would be inappropriate for real-world applications. Stress and displacement of FG hollow cylinder are reported at an angular velocity ( $\omega$ ) = 50 rps. Furthermore, the analysis was extended for FG hollow cylinder under the influence of rotation, gravitational force, and varying internal heat generation.

Stress distribution along the radial direction of the cylinder is investigated by the von Mises stress  $\sigma^* = \sqrt{2}|\sigma_r - \sigma_\theta|$  for different values of the power law material index [42].

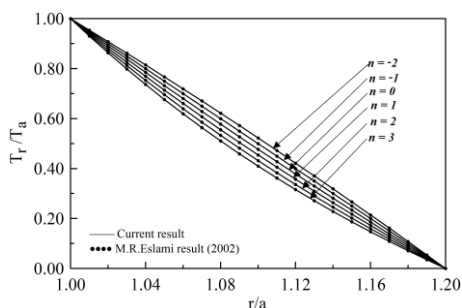


Fig. 6 Radially distributed temperature

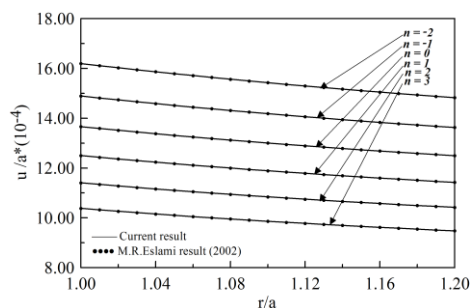


Fig. 7 Radially distributed displacement

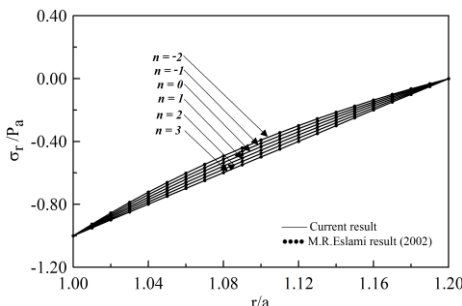


Fig. 8 Radially distributed radial stress

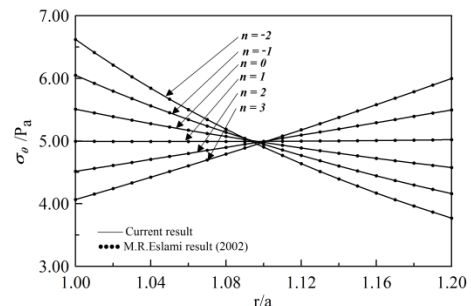


Fig. 9 Radially distributed tangential stress

Fig. 6 shows a decrease in  $T_r/T_a$  ratio from the inner to the outer radius of the cylinder. Temperature distribution and displacement are plotted for an index value of -2 to 3 as shown, whereas the negative value of the index shows a higher value of temperature & displacement as compared to the positive value of the index value.

For the negative value of the grading parameter, the magnitude of temperature is higher compared to the positive value of grading parameters. Fig. 7 to Fig. 9 show the radial displacement, radial stress, and tangential stress for aspect ratio  $b/a = 1.2$ . It is clear that the displacement decreases from the inner to outer radius, the magnitude is maximum for the negative grading parameter and minimum for the positive grading parameter, and least for indices,  $n = 3$ . The radial stress is maximum for the negative grading index and minimum for the positive grading index. Similarly, the tangential stress is maximum at the inner radius and for a negative grading index i.e.,  $n < 1$ , a reverse trend is seen beyond,  $(r/a) = 1.10$  and so the tangential stress reaches a maximum value at  $r/a = 1.20$  for positive grading index i.e.,  $n > 1$ .

### 3.3 Effect of Rotation in a Hollow Cylindrical Body

Fig. 10-14 shows the distribution of temperature, displacement, radial stress, tangential, and von Mises stress due to rotation effect only. Because of the rotational effect on the cylindrical body, the displacement and stresses induced are higher compared to the non-rotating case. Displacement is higher for a negative value of  $n$  as compared to a positive value of  $n$ . Radial stress is also higher for the negative value of  $n$  as compared to the positive value of  $n$  and compressive throughout the radial direction. For a negative value of  $n$ , the tangential and von Mises stresses are higher at the inner radius and then start converging up to  $r/a = 1.08$  (approximately), after that tangential and von Mises stresses are diverging in nature. Stresses and displacement are higher due to the influence of rotation which can be seen when comparing the respective figures of section 3.2 with section 3.3. This analysis proposed an idea for a rotating hollow cylindrical body.

### 3.4 Effect of Gravity in Hollow Cylindrical Body

Fig. 15-19 shows the distribution of temperature, displacement, radial stress, tangential, and von Mises stress due to the gravity effect only. The maximum displacement attained is lesser than rotation. The nature of the variation of displacement and stresses is similar to that obtained in the previous case (section 3.3). Due to the effect of gravity, the results of displacement and stresses are lesser.

### 3.5 Effect of Variable Heat Generation in a Cylindrical Body

Fig. 20-24 shows the distribution of temperature, displacement, radial stress, tangential, and von Mises stress due to the variable heat generation effect. Fig. 20 shows the temperature distribution along the radial direction with variable heat generation. Here, the relationship between displacement and material grading index is inversely proportional i.e. for a negative value of  $n$ , the displacement is higher as compared to the positive value of  $n$ . The relation between displacement and radius of a hollow cylindrical body is inverse i.e. displacement is higher at  $r=0$  and decreases as  $r$  increases.

The relation between radial stress and grading index is inversely proportional i.e. for a negative value of  $n$  radial stress is higher as compared to the positive value of  $n$ , the nature of tangential stress and von Mises stress is similar to the previous cases (section 3.3) but the magnitude is lesser. The results obtained in this case are higher as compared to the reference due to the influence of variable heat generation which is visible when comparing the figure of section 3.2 with section 3.5. This analysis proposed an idea for a hollow cylindrical body with variable heat generation.

### 3.6 Effect of rotation and gravity in cylindrical body

Fig. 25-29 shows the distribution of temperature, displacement, radial stress, tangential, and von Mises stress due to the influence of rotation and gravity together. The result obtained for displacement and stresses are similar to the result obtained in section 3.3 but the magnitude obtained is less as compared to section 3.3 (only rotation) because of

the combined influence of rotation & gravity. Magnitude is higher because of the influence of rotation & gravity. This analysis proposed an idea for hollow cylindrical body under the influence of rotation and gravity.

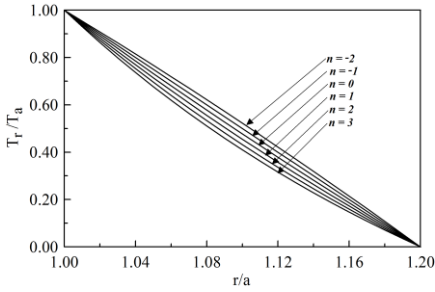


Fig. 10 Temperature distribution

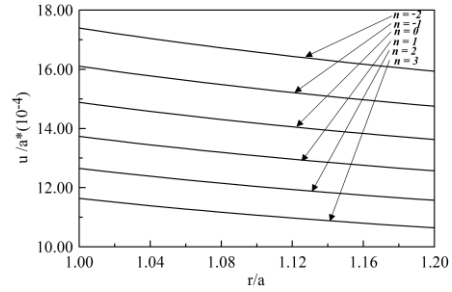


Fig. 11 Displacement results

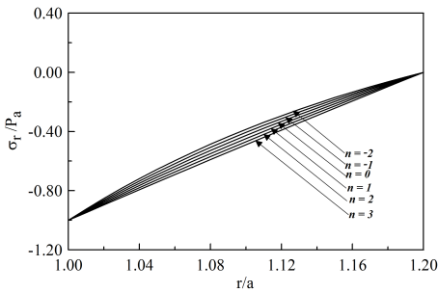


Fig. 12 Radial stress distribution

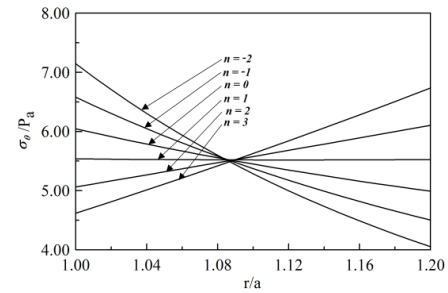


Fig. 13 Tangential stress distribution

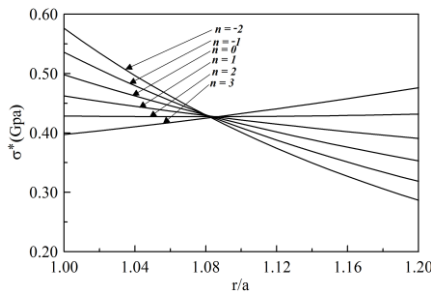


Fig. 14 von Mises stress along radial direction

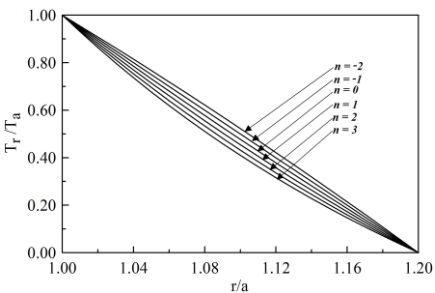


Fig. 15 Temperature distribution

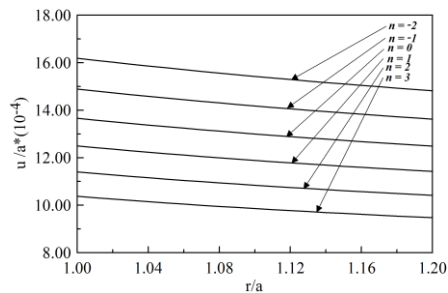


Fig. 16 Displacement results

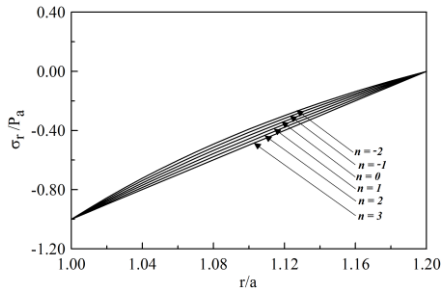


Fig. 17 Radial stress distribution

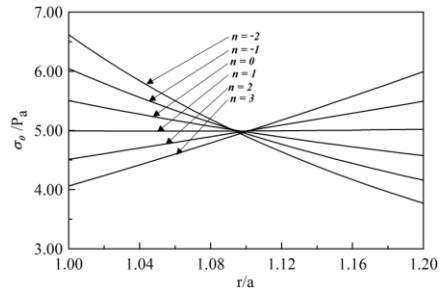


Fig. 18 Tangential stress distribution

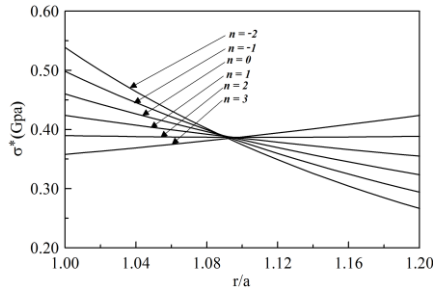


Fig. 19 von Mises results along radial direction

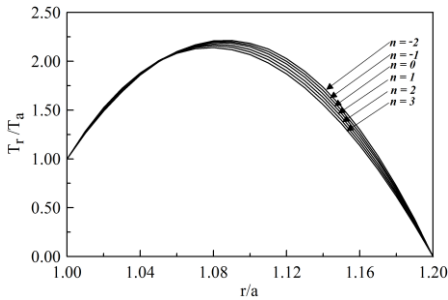


Fig. 20 Temperature distribution

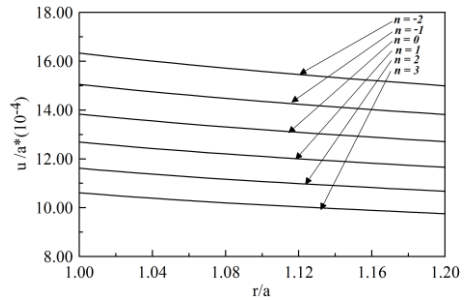


Fig. 21 Displacement results

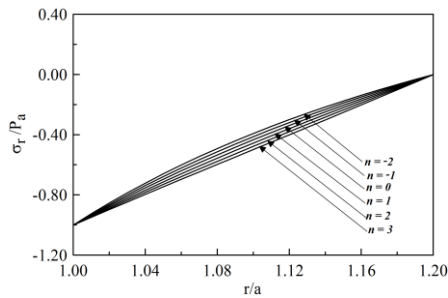


Fig. 22 Radial stress distribution

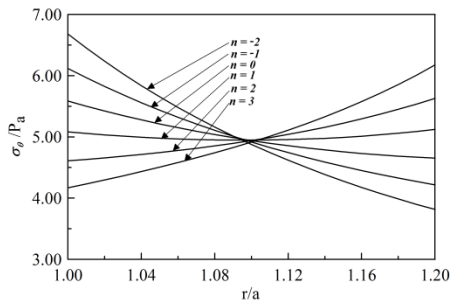


Fig. 23 Tangential stress distribution

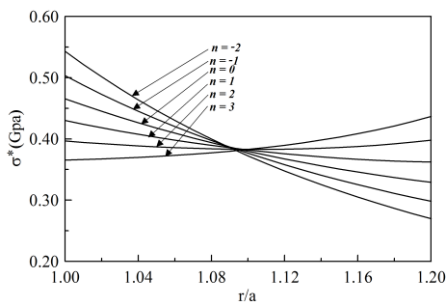


Fig. 24 von Mises results along radial direction

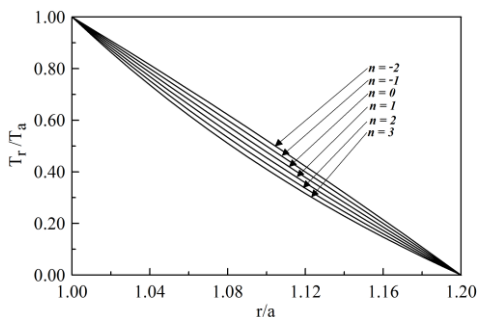


Fig. 25 Temperature distribution

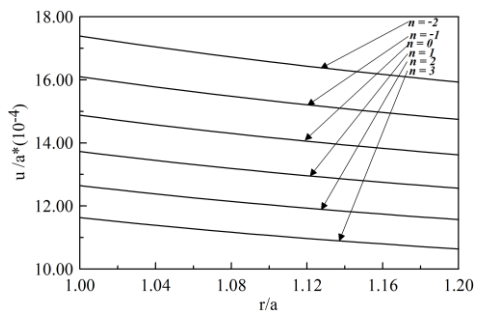


Fig. 26 Displacement results

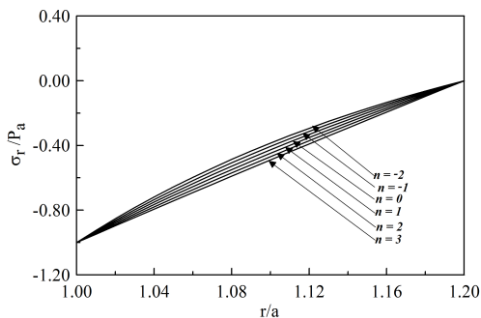


Fig. 27 Radial stress distribution

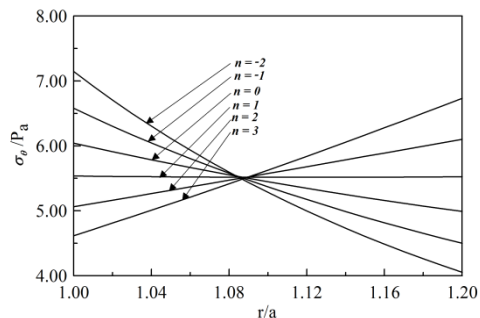


Fig. 28 Tangential stress distribution

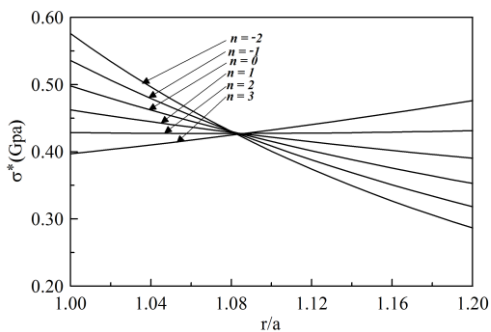


Fig. 29 von Mises results along radial direction

### 3.7 Effect of Rotation and Variable Heat Generation in a Cylindrical Body

Fig. 30-34 shows the distribution of temperature, displacement, radial stress, tangential, and von Mises stress due to rotation and variable heat generation. The nature of variation of displacement and stresses along the radius is similar to the previous cases and the relation of grading index with displacement and stresses is also similar to that discussed in previous cases. Due to the combined influence of rotation and variable heat generation, the result of displacement and stresses are higher compared to the previous cases. The combined effect of rotation and variable heat generation is visible when comparing the figures of sections 3.2, 3.3, 3.4, 3.5, and 3.6 with this present section. The variation of temperature is abrupt along the radius. This analysis proposed the idea of a hollow cylindrical body with the influence of rotation and heat generation.

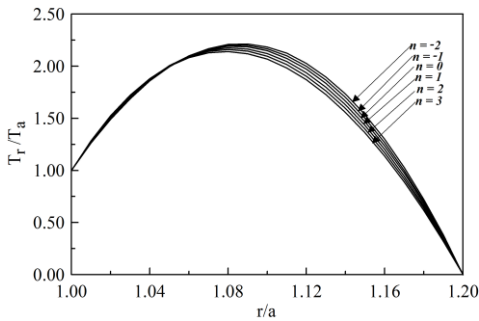


Fig. 30 Temperature distribution

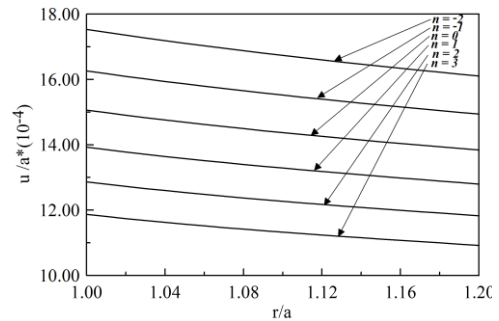


Fig. 31 Displacement results

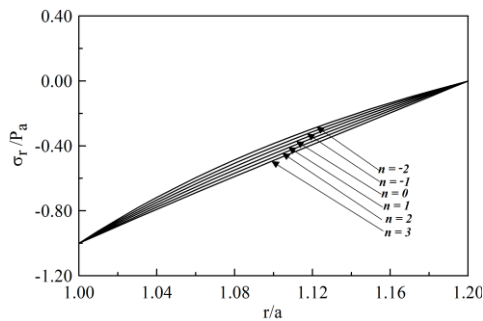


Fig. 32 Radial stress distribution

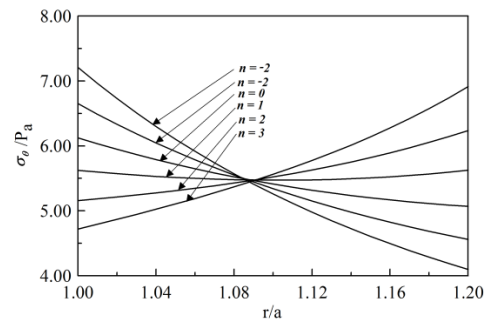


Fig. 33 Tangential stress distribution

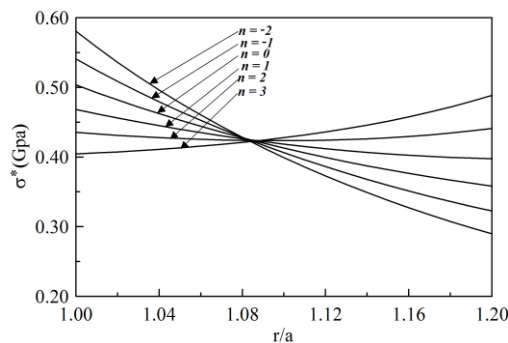


Fig. 34 von Mises results along radial direction

### 3.8 Effect of Gravity and Variable Heat Generation in Hollow Cylindrical Body

Fig. 35-39 shows the distribution of temperature, displacement, radial stress, tangential, and von Mises stress due to gravity and variable heat generation. Due to the combined loading of gravity and heat generation the results are less as compared to sections 3.3, 3.5, 3.6, and 3.7 but higher as compared to the reference & section 3.4 while comparing the figures. So this analysis proposed an idea of hollow cylindrical body influenced by gravity and variable heat generation.

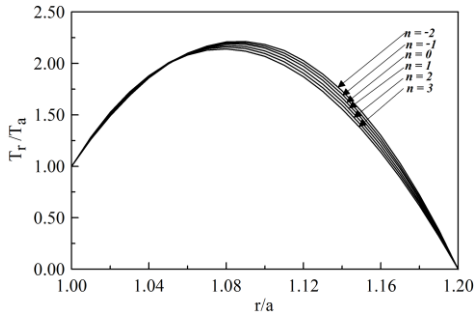


Fig. 35 Temperature distribution

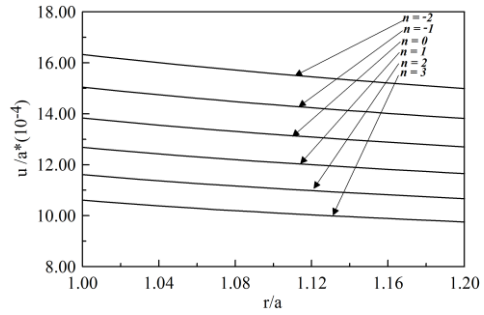


Fig. 36 Displacement results

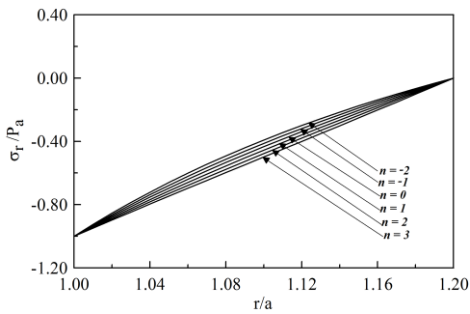


Fig. 37 Radial stress distribution

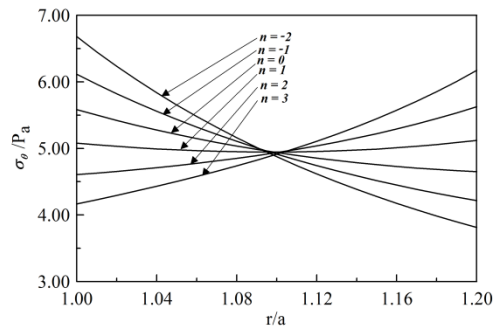


Fig. 38 Tangential stress distribution

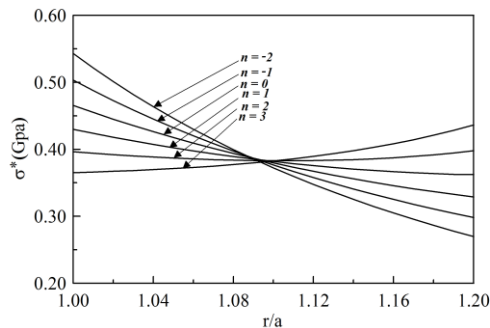


Fig. 39 von Mises results along radial direction

### 3.9 Effect of Rotation, Gravity and Variable Heat Generation in Hollow Cylindrical Body

Fig. 40-44 shows the distribution of temperature, displacement, radial stress, tangential, and von Mises stress due to rotation, gravity, and variable heat generation. In all the cases, the negative value of the grading index shows a higher value of radial stress as compared to the positive grading index. A reverse trend is seen in the variation of tangential stress along the radius, i.e., the tangential stress is converging type at the beginning and becomes equal at the center ( $r/a=1.09$  approx.) irrespective of the grading parameter. Beyond this, the tangential stress shows a diverging behavior. In the converging part, the negative index yields a higher value of tangential stress as compared to the positive value of the index. The von Mises stress distribution is plotted in the radial direction from the inner side to the outer surface of the cylinder. The von Mises stresses are convergent up to the mid-surface after reaching a critical point and then the trend reverses. The nature of the convergent and divergent von Mises stress is similar to that of tangential stress distribution. The result obtained is higher as compared to the reference and all above sections except section 3.7 which is observed when comparing the results of all sections discussed in this paper. So, this analysis proposed the idea of a hollow cylindrical body combined with rotation, gravity, and variable heat generation.

A power-law variation of material property is considered in the present study. The power law is applied directly to the material properties and not to the volume fraction variation of functionally graded materials. The other aspect of analyzing these structures is layer-wise or continuously graded. The difference between these two methods is that in a layer-wise structure the stress distribution obtained is discontinuous and stress jumps can be seen at the interface. On the other hand, when the change in material composition is smoother there will be no jump at the interface. It is always preferred to vary the composition in a smoother fashion such that the causes of delamination can be prohibited which may arise due to the difference in thermo-mechanical properties of a material selected for the fabrication of functionally graded structures. The distribution of stresses varies smoothly along the radial direction. And so, the selection of grading parameters plays a crucial role in improving the performance of functionally graded materials.

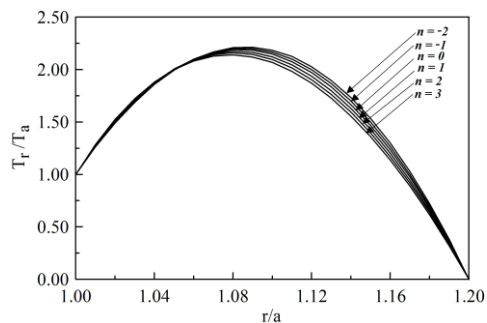


Fig. 40 Temperature distribution

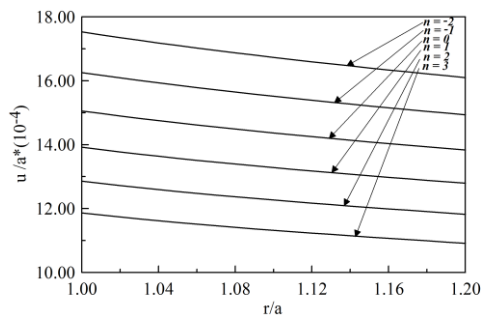


Fig. 41 Displacement results

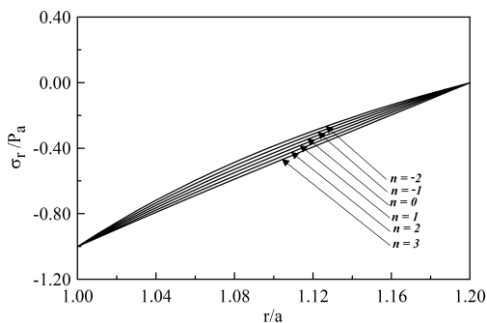


Fig. 42 Radially Distributed Radial Stress

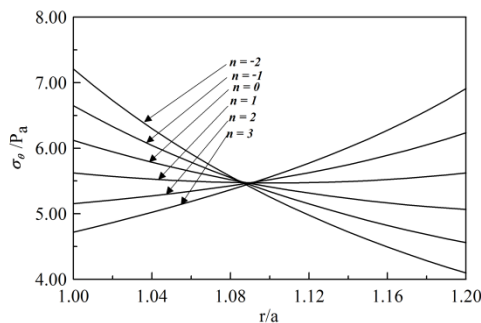


Fig. 43 Tangential stress distribution

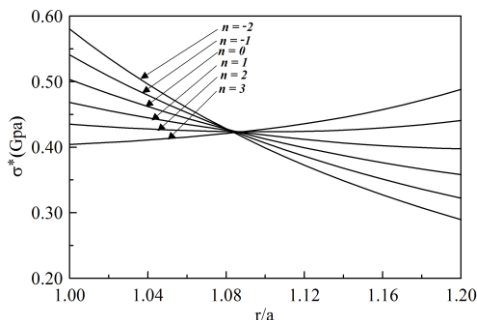


Fig. 44 von Mises results along radial direction

#### 4. Conclusion

Thermo-mechanical stress analysis of the FG hollow cylinder has been performed for varying grading indices under the effect of grading parameters, rotational speed, gravitational force, and heat generation. By employing Navier’s method, the problem was solved considering variable heat generation in a cylinder.

- The fabrication of such structures is possible using centrifugal casting and additive manufacturing techniques; the centrifugal casting technique is very well suited for fabricating axisymmetric structures whereas there are no such limitations in additive manufacturing. In centrifugal casting, the gradation variation will be continuous whereas in additive manufacturing because of layer-wise deposition a layer-wise gradation is expected.
- Due to the increments in grading parameters, the strength of the hollow cylindrical body is improving resulting in lowering the displacement and radial stresses. The von Mises stresses decrease till a certain value of  $b/a$  is reached beyond this von Mises stresses of FG hollow cylindrical body increase. The magnitude of von-Mises stress is higher at the inner radius of FG hollow cylindrical body and lesser at the outer radius, but for  $n = 3$  the variation in von Mises stress is almost uniform.
- For  $n > 1$ , the tangential stresses of FG hollow cylindrical body increase radially but for  $n < 1$ , it decreases; and for  $n = 1$ , the variation in tangential stress is almost uniform along the radial direction.
- From the analysis of the hollow cylindrical body, it was found that the radial displacement varies inversely with the grading index whereas the tangential stress increases with  $n$  when  $n$  is greater than unity. Similarly, von Mises stress

is directly proportional to a grading index greater than 2 and inversely to a grading index less than 2.

### Nomenclature

$a$	Inner radius (m)	$\rho_r$	Density function ( $kg/m^3$ )
$b$	Outer radius (m)	$q_r$	Heat generation function ( $kJ/m^3$ )
$r$	Radial direction (m)	$E_a$	Young's modulus at 'a' (MPa)
$u$	Displacement component (m)	$\alpha_a$	CTE at 'a' (per °C)
$\epsilon_r$	Radial strain	$k_a$	TCC at 'a' (W/mk)
$\epsilon_\theta$	Tangential strain	$\rho_a$	Density at 'a' ( $kg/m^3$ )
$\sigma_r$	Radial stress (MPa)	$q_a$	Heat generation at 'a' ( $kJ/m^3$ )
$\sigma_\theta$	Tangential stress (MPa)	$n_1, n_2, n_3, \gamma$	Material index
$u', T'$	1 <sup>st</sup> order differential	$T_r$	Temperature function (°C)
$u'', T''$	2 <sup>nd</sup> order differential	$T_a$	Temperature at 'a' (°C)
$\omega$	Rotation (rad/s)	$T_b$	Temperature at 'b' (°C)
$g$	Gravity ( $m/s^2$ )	$Q_3, Q_4,$ $P_3, P_4$	Thermal constants
$E_r$	Young's modulus function (MPa)	$Q_1, Q_2,$ $P_1, P_2$	Displacement constants
$\alpha_r$	CTE function (per °C)	$P_a$	Pressure at inside (MPa)
$k_r$	Thermal conduction coefficient (TCC) function (W/mk)	$P_b$	Pressure at outside (MPa)

### References

- [1] Saleh B, Jiang J, Ma A, et al. Review on the Influence of Different Reinforcements on the Microstructure and Wear Behavior of Functionally Graded Aluminum Matrix Composites by Centrifugal Casting. *Met Mater Int* 2020; 26: 933-960. <https://doi.org/10.1007/s12540-019-00491-0>
- [2] Mortensen A, Suresh S. Functionally graded metals and metal-ceramic composites: Part 1 Processing. *Met Mater Int* 1995; 40: 239-265. <https://doi.org/10.1179/imr.1995.40.6.239>
- [3] Madan R, Bhowmick S. A review on application of FGM fabricated using solid-state processes. *Advances in Materials and Processing Technologies* 2020; 6: 608-619. <https://doi.org/10.1080/2374068X.2020.1731153>
- [4] Parihar RS, Setti SG, Sahu RK. Recent advances in the manufacturing processes of functionally graded materials: a review. *Science and Engineering of Composite Materials* 2018; 25: 309-336. <https://doi.org/10.1515/secm-2015-0395>
- [5] Saleh B, Jiang J, Fathi R, et al. 30 Years of functionally graded materials: An overview of manufacturing methods, Applications and Future Challenges. *Composites Part B: Engineering* 2020; 201: 108376. <https://doi.org/10.1016/j.compositesb.2020.108376>
- [6] Verma RK, Parganiha D, Chopkar M. A review on fabrication and characteristics of functionally graded aluminum matrix composites fabricated by centrifugal casting method. *SN Appl Sci* 2021; 3: 227. <https://doi.org/10.1007/s42452-021-04200-8>

- [7] Abdalla HMA, Casagrande D, De Bona F, et al. An optimized pressure vessel obtained by metal additive manufacturing: Preliminary results. *International Journal of Pressure Vessels and Piping* 2021; 192: 104434. <https://doi.org/10.1016/j.ijpvp.2021.104434>
- [8] Arefi M, Firouzeh S, Mohammad-Rezaei Bidgoli E, et al. Analysis of porous micro-plates reinforced with FG-GNPs based on Reddy plate theory. *Composite Structures* 2020; 247: 112391. <https://doi.org/10.1016/j.compstruct.2020.112391>
- [9] Lakshman S, Subhashis S, Kashinath S, et al. Limit elastic speeds of functionally graded annular disks. *FME Transactions* 2018; 46: 603-611. <https://doi.org/10.5937/fmet1804603S>
- [10] Madan R, Bhowmick S. A numerical solution to thermo-mechanical behavior of temperature dependent rotating functionally graded annulus disks. *AEAT*; ahead-of-print. Epub ahead of print 7 June 2021. <https://doi.org/10.1108/AEAT-01-2021-0012>
- [11] Madan R, Bhowmick S. Modeling of functionally graded materials to estimate effective thermo-mechanical properties. *WJE*; ahead-of-print. Epub ahead of print 26 January 2021. DOI: 10.1108/WJE-09-2020-0445. <https://doi.org/10.1108/WJE-09-2020-0445>
- [12] Sharma D, Kaur R. Thermoelastic analysis of FGM hollow cylinder for variable parameters and temperature distributions using FEM. *Nonlinear Engineering* 2020; 9: 256-264. <https://doi.org/10.1515/nleng-2020-0013>
- [13] Bacciocchi M, Luciano R, Majorana C, et al. Free Vibrations of Sandwich Plates with Damaged Soft-Core and Non-Uniform Mechanical Properties: Modeling and Finite Element Analysis. *Materials* 2019; 12: 2444. <https://doi.org/10.3390/ma12152444>
- [14] Menasria A, Kaci A, Bousahla AA, et al. A four-unknown refined plate theory for dynamic analysis of FG-sandwich plates under various boundary conditions. *Steel and Composite Structures* 2020; 36: 355-367.
- [15] Liang K, Li Z. A novel nonlinear FE perturbation method and its application to stacking sequence optimization for snap-through response of cylindrical shell panel. *Computers & Mathematics with Applications* 2022; 112: 154-166. <https://doi.org/10.1016/j.camwa.2022.03.002>
- [16] Chen Z-F, Wang H-J, Sang Z, et al. Theoretical and Numerical Analysis of Blasting Pressure of Cylindrical Shells under Internal Explosive Loading. *JMSE* 2021; 9: 1297. <https://doi.org/10.3390/jmse9111297>
- [17] Ozturk A, Gulgec M. Elastic-plastic stress analysis in a long functionally graded solid cylinder with fixed ends subjected to uniform heat generation. *International Journal of Engineering Science* 2011; 49: 1047-1061. <https://doi.org/10.1016/j.ijengsci.2011.06.001>
- [18] Tutuncu N, Temel B. A novel approach to stress analysis of pressurized FGM cylinders, disks and spheres. *Composite Structures* 2009; 91: 385-390. <https://doi.org/10.1016/j.compstruct.2009.06.009>
- [19] Çelebi Kavdir E, Aydin MD. The stress analysis on two different adhesively bonded t-joints via 3d nonlinear finite element method. *Journal of Thermal Engineering* 2020; 170-179. <https://doi.org/10.18186/thermal.729864>
- [20] Trung KN. The temperature distribution of the wet cylinder liner of v-12 engine according to calculation and experiment. *Journal of Thermal Engineering* 2021; 7: 1872-1884. <https://doi.org/10.18186/thermal.1051265>
- [21] Falsonea G, La Valle G. Dynamic and buckling of functionally graded beams based on a homogenization theory. *Res. Eng. Struct. Mater.*, 2021; 7(4): 523-538. <https://doi.org/10.17515/resm2021.259st0216>
- [22] Esener E, Unlu A. Analytical evaluation of plasticity models for anisotropic materials with experimental validation. *Res. Eng. Struct. Mater.*, 2022; 8(1): 75-89.

- [23] Tutuncu N. Stresses in thick-walled FGM cylinders with exponentially-varying properties. *Engineering Structures* 2007; 29: 2032-2035. <https://doi.org/10.1016/j.engstruct.2006.12.003>
- [24] Ghannad M, Rahimi GH, Nejad MZ. Elastic analysis of pressurized thick cylindrical shells with variable thickness made of functionally graded materials. *Composites Part B: Engineering* 2013; 45: 388-396. <https://doi.org/10.1016/j.compositesb.2012.09.043>
- [25] Jabbari M, Bahtui A, Eslami MR. Axisymmetric mechanical and thermal stresses in thick short length FGM cylinders. *International Journal of Pressure Vessels and Piping* 2009; 86: 296-306. <https://doi.org/10.1016/j.ijpvp.2008.12.002>
- [26] Rahimi GH, Arefi M, Khoshgoftar MJ. Application and analysis of functionally graded piezoelectrical rotating cylinder as mechanical sensor subjected to pressure and thermal loads. *Appl Math Mech-Engl Ed* 2011; 32: 997-1008. <https://doi.org/10.1007/s10483-011-1475-6>
- [27] Khoshgoftar MJ, Rahimi GH, Arefi M. Exact solution of functionally graded thick cylinder with finite length under longitudinally non-uniform pressure. *Mechanics Research Communications* 2013; 51: 61-66. <https://doi.org/10.1016/j.mechrescom.2013.05.001>
- [28] Nejad MZ, Jabbari M, Ghannad M. Elastic analysis of axially functionally graded rotating thick cylinder with variable thickness under non-uniform arbitrarily pressure loading. *International Journal of Engineering Science* 2015; 89: 86-99. <https://doi.org/10.1016/j.ijengsci.2014.12.004>
- [29] Shi Z, Zhang T, Xiang H. Exact solutions of heterogeneous elastic hollow cylinders. *Composite Structures* 2007; 79: 140-147. <https://doi.org/10.1016/j.compstruct.2005.11.058>
- [30] Habib E-S, El-Hadek MA, El-Megharbel A. Stress Analysis for Cylinder Made of FGM and Subjected to Thermo-Mechanical Loadings. *Metals* 2018; 9: 4. <https://doi.org/10.3390/met9010004>
- [31] Peng XL, Li XF. Thermoelastic analysis of a cylindrical vessel of functionally graded materials. *International Journal of Pressure Vessels and Piping* 2010; 87: 203-210. <https://doi.org/10.1016/j.ijpvp.2010.03.024>
- [32] Saeedi S, Kholdi M, Loghman A, et al. Thermo-elasto-plastic analysis of thick-walled cylinder made of functionally graded materials using successive approximation method. *International Journal of Pressure Vessels and Piping* 2021; 194: 104481. <https://doi.org/10.1016/j.ijpvp.2021.104481>
- [33] Yang W, Pang J, Wang L, et al. Thermo-mechanical fatigue life prediction based on the simulated component of cylinder head. *Engineering Failure Analysis* 2022; 135: 106105. <https://doi.org/10.1016/j.engfailanal.2022.106105>
- [34] M. Dehghan. An Approximate Thermo-Mechanical Solution of a Functionally Graded Cylinder Using Hybrid Integral Transform and Finite Element Method. *Journal of Solid Mechanics* 2022; 14: 17-36.
- [35] Chen YZ, Lin XY. Elastic analysis for thick cylinders and spherical pressure vessels made of functionally graded materials. *Computational Materials Science* 2008; 44: 581-587. <https://doi.org/10.1016/j.commatsci.2008.04.018>
- [36] Go J, Afsar AM, Song JI. Analysis of Thermoelastic Characteristics of a Rotating FGM Circular Disk by Finite Element Method. *Advanced Composite Materials* 2010; 19: 197-213. <https://doi.org/10.1163/092430410X490473>
- [37] Frahlia H, Bennai R, Nebab M, et al. Assessing effects of parameters of viscoelastic foundation on the dynamic response of functionally graded plates using a novel HSDT theory. *Mechanics of Advanced Materials and Structures* 2022; 1-15. <https://doi.org/10.1080/15376494.2022.2062632>

- [38] Bennai Riadh, Mellal Fatma, Nebab Mokhtar, et al. On wave dispersion properties of functionally graded plates resting on elastic foundations using quasi-3D and 2D HSDT. *Earthquakes and Structures* 2022; 22: 447-460.
- [39] Mellal F, Bennai R, Nebab M, et al. Investigation on the effect of porosity on wave propagation in FGM plates resting on elastic foundations via a quasi-3D HSDT. *null* 2021; 1-27. <https://doi.org/10.1080/17455030.2021.1983235>
- [40] Nebab M, Ait Atmane H, Bennai R, et al. Effect of variable elastic foundations on static behavior of functionally graded plates using sinusoidal shear deformation. *Arab J Geosci* 2019; 12: 809. <https://doi.org/10.1007/s12517-019-4871-5>
- [41] Jabbari M, Sohrabpour S, Eslami MR. Mechanical and thermal stresses in a functionally graded hollow cylinder due to radially symmetric loads. *International Journal of Pressure Vessels and Piping* 2002; 5. [https://doi.org/10.1016/S0308-0161\(02\)00043-1](https://doi.org/10.1016/S0308-0161(02)00043-1)
- [42] Eslami MR, Babaei MH, Poultangari R. Thermal and mechanical stresses in a functionally graded thick sphere. *International Journal of Pressure Vessels and Piping* 2005; 82: 522-527. <https://doi.org/10.1016/j.iijpvp.2005.01.002>